ZOOLOGICAL SCIENCE **22**: 1145–1156 (2005)

Generation of Knock-in Mice Carrying Third Cones with Spectral Sensitivity Different from *S* and *L* Cones

Akishi Onishi[1,2], Jun Hasegawa[3], Hiroo Imai[1,2], Osamu Chisaka[4], Yoshiki Ueda[5†], Yoshihito Honda[5‡], Masao Tachibana[3] and Yoshinori Shichida[1,2*]

[1]*Department of Biophysics, Graduate School of Science, Kyoto University, Kyoto 606-8502, Japan*
[2]*Core Research for Evolutional Science and Technology (CREST), Japan Science and Technology Agency*
[3]*Department of Psychology, Graduate School of Humanities and Sociology, The University of Tokyo, Tokyo 113-0033, Japan*
[4]*Department of Cell and Developmental Biology, Graduate School of Biostudies, Kyoto University, Kyoto 606-8502, Japan*
[5]*Department of Ophthalmology and Visual Sciences, Graduate School of Medicine, Kyoto University, Kyoto 606-8507, Japan*

ABSTRACT—Red-green color vision in primates is unique in the sense that it is mediated by two photoreceptor cells that are indistinguishable in all aspects except for their visual pigments. In order to generate an animal model for investigation of the interaction between red-green inputs at the molecular level, we applied knock-in technology and X-chromosome inactivation machinery to make a mouse model with cone cells possessing visual pigments with different spectral sensitivities. We introduced a S308A point mutation into the Green opsin gene allele on the X-chromosome. This manipulation generated a 24 nm red-shift of absorption maximum in the cone pigment with negligible functional differences in other molecular properties. Amplitudes of responses in ERG and ganglion cell recordings of homozygotes were similar to those of wild-types, although the spectral sensitivities differed. Heterozygotes showed variable spectral sensitivities of ganglion cell responses due to the different integration of the native and the S308A cone inputs on the dendritic fields. *In situ* hybridization experiments showed that cone cells with respective pigments formed patch-like clusters of specific *L* cone-types, approximately 30 μm in diameter, which were randomly distributed in the dorsal region of the retinas. Since the patch-like clustering was arranged by X-inactivation, such clustering could be present in the peripheral retinas of New World monkeys with polymorphic *L* pigments, indicating that our mice would be a suitable model to study evolution of the mammalian color vision system.

Key words: spectral tuning, X-inactivation, cone pigments, knock-in mice, color vision

INTRODUCTION

Color processing in vertebrates begins with integration of inputs from cone cells of different spectral sensitivities by subsequent neural cells. Because the spectral responses of the cone cells reflect the spectral sensitivities of the visual pigments in the cells, color discrimination depends on the number of visual pigments with distinct spectral sensitivities present in different kinds of photoreceptor cells. Vertebrate cone pigments have diverged into four groups (*S*, M_1, M_2, and *L*) during the course of molecular evolution, and each group contains visual pigments whose absorption maxima are quite similar to each other but different from those of other groups (Okano *et al*., 1992). Most vertebrates, from ichthyoids to avians, have four cone pigments belonging to each group, and are thought to have tetrachromatic (or trichromatic) color vision. On the other hand, most mammals have only two kinds of cone pigments that belong to the *S* and *L* groups. Old World and some New World primates recruited trichromatic color vision by duplicating the *L* visual pigment gene during the course of evolution (for reviews, see Tovée, 1994). Furthermore, color opponent signals can be generated in horizontal cells in lower vertebrates (for

* Corresponding author. Phone: +81-75-753-4213;
Fax : +81-75-753-4210;
E-mail: shichida@vision-kyoto-u.jp
† Present address: Nagahama City Hospital, Nagahama, Shiga 526-8380, Japan
‡ Present address: Osaka Red Cross Hospital, Osaka 543-5111, Japan

recent reviews, see Twig *et al.*, 2003) and in ganglion cells in mammals (Wienrich and Zrenner, 1984; Hemmi *et al.*, 2002). Therefore, changes in the number of photoreceptor cells with distinctive spectral sensitivities during the course of vertebrate evolution could dynamically modify the neural network systems that govern color discrimination.

In Old World primates that have recovered trichromatic color vision, the outputs from the *S* (Blue) cone cells and the summation of the two *L* (Red and Green) cone cells are processed by the morphologically distinctive synaptic junctions (Dacey and Lee, 1994; Dacey, 1996; Calkins *et al.*, 1998). However, except for their visual pigments, the Red and Green cone cells are indistinguishable in all aspects, namely, morphology, physiology, retinal distribution and so on (Mariani, 1984; Schneeweis and Schnapf, 1999; Roorda *et al.*, 2001). This situation is more prominent in New World primates. In contrast to Old World primates in which each X-chromosome carries two kinds of *L* (Red and Green) genes in a tandem arrangement, most New World primates have only a single *L* gene on one X-chromosome. However, the *L* gene is highly polymorphic in spectral sensitivity so that females with polymorphic *L* genes in each X-chromosome exhibit red-green color discrimination (Tovée, 1994; Jacobs *et al.*, 1996). These results emphasize that in primate red-green color vision, the same types of photoreceptor cells exhibiting differences in spectral sensitivities of visual pigments can contribute to formation of a network system for Red-Green color discrimination. Thus it is of interest to investigate the mechanism by which inputs of similar cone cells can be converted to signals of color discrimination. For this purpose, we have been studying visual systems in protanopic macaque monkeys that have a Blue gene and a single Red-Green hybrid genes (Onishi *et al.*, 1999, 2002; Hanazawa *et al.*, 2001), and protanomalia chimpanzees that have a Blue gene, a Green gene, and a single Red-Green hybrid genes (Saito *et al.*, 2003; Terao *et al.*, 2005). A similar approach has been performed in New World primates (Jacobs and Neitz, 1985; Ghosh *et al.*, 1996; Jacobs *et al.*, 1996; Wilder *et al.*, 1996; Goodchild and Martin, 1998; Chan *et al.*, 2001; Solomon, 2002). However, primates would not be suitable for investigation at a molecular level, partly because of lower fertility and longer generation time.

In this study, we attempted to generate an animal model in order to study the processing mechanism of color signals from two cone photoreceptor cells of identical physiological, morphological and genetic backgrounds but carrying visual pigments with only different spectral sensitivities. For this purpose, we used knock-in technology to generate mice expressing a visual pigment that exhibited an absorption maximum different from that present in the native Green cone cells. Since wild-type mice have a single X-linked *L* gene (Green gene), we generated our model by mimicking the allelic trichromacy seen in New World primates. We attempted to generate a cone pigment having a different absorption maximum by introducing a single amino acid substitution into the exon region of the Green gene allele, because replacement that does not disturb the exon-intron arrangement is supposed to lead to similar transcription and translation as seen in the wild-type. We further examined the molecular properties of the mutant pigment before generating mice with this pigment in their retinas. Our biophysical experiments clearly showed that the S308A point mutant exhibited an absorption maximum 24 nm red-shifted from the wild-type pigment (Sun *et al.*, 1997), but retained its other molecular properties, including photosensitivity, hydroxylamine sensitivity, G-protein activation rate, and lifetime of the meta-II intermediate, characteristic of cone pigments as compared to the rod pigment, rhodopsin (Shichida and Imai, 1998). On the other hand, we introduced a 37 bp silent mutation neighboring the S308A mutation site to discriminate the wild-type and mutant mRNAs for *in situ* hybridization. The results clearly showed that the newly introduced gene was expressed at similar quantities but in different photoreceptor cells as a result of X-chromosome inactivation. Combined with the results obtained by electrophysiology, *in situ* hybridization and immunostaining, the suitability of this mouse model for investigation of red-green color vision in primates is discussed.

MATERIALS AND METHODS

Spectroscopy

Mouse rhodopsin, UV, and Green pigments (wild-type: mGWT and S308A: mGS308A) were expressed in the HEK293T cell lines, as previously reported (Imai *et al.*, 2000). These pigments, with the exception of the rhodopsin, were tagged with an 1D4 epitope sequence (8-aa C-terminal of bovine rhodopsin; ETSQVAPA). The expressed pigments were regenerated by incubation with 11-*cis*-retinal, extracted by 0.75% CHAPS/0.8 mg/ml PC buffer (50 mM HEPES, 140 mM NaCl, and 1 mM $MgCl_2$, pH 6.5), and purified with an 1D4 antibody-conjugated column. The UV-vis absorption spectra were recorded using a Shimadzu Model MPS-2000 spectrophotometer interfaced with an NEC PC-9801 computer. The thermal conversion rates from meta-II to meta-III intermediates of wild-type and S308A Green pigments were monitored at 2°C, as previously reported (Kuwayama *et al.*, 2002). Namely, the absorption spectra were continuously measured after 3 second irradiation with λ>510 nm and λ>540 nm light for the wild-type and S308A pigments, respectively. Hydroxylamine sensitivity was determined by the addition of 100 mM hydroxylamine to the pigments at 20°C under dark conditions; spectra were subsequently recorded at several time points.

G-protein activation assays

Light-induced activations of bovine rod transducin by rhodopsin, mGWT and mGS308A were measured using a GTPγS-binding assay at 4°C, as described previously (Terakita *et al.*, 1998; Das *et al.*, 2004). Mouse rhodopsin, mGWT and mGS308A were extracted with 0.1% dodecyl maltoside in buffer Pm (50 mM HEPES, 140 mM NaCl and 1 mM $MgCl_2$, pH 6.5) and were purified with a 1D4 antibody-conjugated column. Pigment concentrations of mGWT and mGS308A were determined by absorption spectroscopy. That is, absorbances at the maxima of the samples were measured and the values were converted to the pigment concentrations by using molecular extinction coefficients (ε_{max}). The ε_{max} s of the pigments were estimated relative to that of bovine rhodopsin (42,700, Hong and Hubbell, 1972; Sakmar *et al.*, 1989) by using an acid-denaturing method (Sakmar *et al.*, 1989). The ε_{max} values of mGWT and

mGS308A relative to the value of rhodopsin were 45,500±2500 and 46,800±2000, respectively, indicating that the mutation caused little difference in the molecular extinction coefficient of the pigment.

The reaction mixture contained 5 nM pigment, 1.25 μM transducin and 3 μM GTPγS in the buffer (0.01% dodecyl maltoside , 50 mM HEPES, 140 mM NaCl and 1 mM $MgCl_2$, pH 6.5) . Immediately after preparation of the mixture, it was irradiated with orange light for 30 s or kept in the dark at 4°C. Then, the sample was incubated for the selected time in the dark, and an aliquot (10 μl) was removed from the sample, added to 250 μl of stop solution (20 mM Tris/Cl, 100 mM NaCl, 25 mM $MgCl_2$, 2 μM GTPγS, pH 7.4), and immediately filtered through a nitrocellulose membrane to trap [^{35}S]GTPγS bound to transducin. The amount of [^{35}S]GTPγS bound to the membrane was quantified with a liquid scintillation counter (LS 6000IC, Beckman).

Generation of knock-in mice

Mouse genomic DNA clones were isolated from the 129SvJ-derived genomic library, and the clones spanning the exon 5 region consisting of codon 308 were used to construct the targeting vector. The exon 5 fragment that contained a S308A point mutation for a spectral shift and a 37 bp silent mutation neighboring the S308A mutation site for the discrimination of native and S308A mRNA was artificially synthesized. For a 5' linker, we used an 11.2 kb genomic segment expanding from the *Eco*RI site on the 3' side of exon 2 to exon 5. At the 3' end (about 1.5 kb upstream of exon 5), a *loxP*-phosphoglycerate kinase promoter-neomycin photosphotranspherase II (PGK-Neo)-*loxP* cassette was inserted for positive selection of electroporated ES cells by G418, a neomycin analogue. For a 3' linker, a 2.7 kb genomic segment expanding from exon 5 to the *Eco*RI site on the 3' side of exon 6 was used. At the 3' end, a herpes simplex virus promoter-thymidine kinase (HSV-tk) cassette was introduced for negative selection by gancyclovir to exclude nonhomologous recombinants of electroporated ES cells. The targeting vector was electroporated to CMTI-1 ES cells (Cell & Molecular Technologies), and the homologous recombinants were selected. The knock-in mice were generated by blastocyst injection of the ES clone (Chisaka and Capecchi, 1991) and were crossed with mice that express Cre recombinase in order to remove the PGK-Neo cassette in the targeted genome. Since a knock-in mouse has 129 backgrounds, backcross was performed to generate knock-in mice of the C57BL/6 background. Mice of ages ranging from 8 to 20 weeks old were used in all of the experiments. The experimental procedure was carried out in accordance with the guidelines set by Kyoto University, and was approved by the local committee for the handling of experimental animals in the Graduate School of Science, Kyoto University.

Electroretinogram (ERG)

The mice were anesthetized with an intraperitoneal injection of a saline solution containing ketamine and xylazine (13 and 86 mg/kg body weight, respectively). Pupils were dilated with 1% tropicamide. Body temperature was maintained near 37°C using a heating pad. An ERG was recorded from the corneal surface with a coiled gold-wire that made contact with a thin layer of 1% methylcellulose (Mears *et al.*, 2001). A similar wire placed in the conjunctival sac and a needle electrode inserted in the tail served as the reference and ground electrodes, respectively. Signals were amplified by an ML135 Dual Bio Amp (ADInstruments Pty Ltd), bandpass-filtered at 0.1–1000 Hz, sampled at 4 kHz, and then stored in a computer.

We elicited photopic cone ERGs on a rod-suppressing 96 cd/m^2 halogen background light which suppressed almost all the rod components but not UV and green cone components (Lyubarsky *et al.*, 1999). It should be noted that the halogen lamp suppressed the green cone response more than the UV cone response because of its spectral characters. To detect a spectral shift that resulted in the S308A knock-in, we utilized 470 nm, 520 nm, and 570 nm monochromatic lights for light stimuli. Spectral sensitivities were significantly different at 470 nm and 570 nm, between Green WT and S308A pigments, while they were equivalent at 520 nm (isosbestic point). Strobe flash stimuli (Nikon, SB-80DX) presented in a Ganzfeld bowl (Mayo Corporation, Nagoya) were limited to 470 nm, 520 nm, and 570 nm, using narrow-band interference filters (normalized half-bandwidth of 10 nm, Edmund). To avoid the time-dependent amplitude change due to the light adaptation of rods and cones, we used stimulation of three monochromatic lights with duration of 20 s. This protocol allowed us to neglect the time-dependent amplitude change but would not allow for the equilibration of photon density for each stimulus. The maximum photon flux densities at the pupil plane for limited light flashes were 157,000, 213,000, and 234,000 photons/μm^2 for 470 nm, 520 nm, and 570 nm stimuli, respectively. We confirmed that the ERG for these lights did show a response amplitude lower than half of the amplitudes of saturated responses (data not shown).

Although photon flux density was not identical among these three stimuli, we compared the spectral sensitivities for 470 nm and 570 nm light stimuli by normalizing the amplitude at the isosbestic point (520 nm). The b-wave amplitudes are dependent on the photoisomerization number ($\Phi(\lambda)$) of the photoreceptors (Lyubarsky *et al.*, 1999). If the amounts of visual pigments are the same between the wild-type and mutant animals, the numbers of the activated wildtype and S308A photoreceptors should be the same at the isosbestic point (λ=520 nm), where the absorption of the two pigments is equivalent. The amplitude ratios (470/520 and 570/520) represented differences in sensitivity for the reference stimuli.

Single cell recordings from retinal ganglion cells

The whole-cell recordings were performed as previously reported (Matsui *et al.*, 2001). The eyes were enucleated, and the dorsal retina was sliced into 200 μm thick sections. The electrode resistance was 6 ~ 9 MΩ in the extracellular control solution (120 mM NaCl, 3.1 mM KCl, 2 mM $CaCl_2$, 1 mM $MgSO_4$, 23 mM $NaHCO_3$, 0.5 mM KH_2PO_4 and 6 mM glucose, saturated with 95% O_2-5% CO_2, pH ~7.6) when pipettes were filled with the intracellular solution (135 mM K-gluconate, 3 mM KCl, 0.5 mM EGTA, 10 mM HEPES, 2.5 mM $MgCl_2$, 2 mM ATP disodium salt, and 0.5 mM GTP and 0.1% Lucifer yellow dipotassium salt, pH 7.6 with KOH). Light-evoked responses were recorded from cells in the ganglion cell layer under whole cell voltage-clamp. In some cells, the recording configuration was switched from the voltage clamp mode to the current clamp mode. Both current and voltage were low-pass-filtered (1 kHz to 5 kHz), digitized at two times the filtering frequency with a digitizer board (Digidata 1200B, Axon Instruments), and then stored in a computer. In order to isolate the cone-driven responses, the slices were continuously illuminated by a 520 nm LED (Toyoda Gosei, E1L53-3G) through a condenser lens and a diffuser to saturate the rod responses. The cone responses were evoked by a high intensity LED (NICHIA Corporation, NSPW500S) through the narrow-band interference filters (λ_{max}: 470 nm, 520 nm, and 570 nm). We measured the light intensities with a Digi-Ana Power Meter PM245 (NEOARK Corporation, Tokyo). The photon flux densities were set to 30,400, 154,000, 153,800, and 154,200 photons/sec/μm^2 for background and 470 nm, 520 nm, and 570 nm for light stimuli. The light flash was applied for 0.5 sec with 1.5 sec inter-stimulus intervals, and several responses were averaged.

***In situ* hybridization and immunostaining**

Digoxigenin-UTP riboprobes specific for the mouse Green wild-type and the S308A mRNA were prepared from the 160 bp region spanning 864–1023 bp that includes the 37 bp silent mutation (see Fig. 2B) of exon 5 and the 5' portion of exon 6. Hybridization of the retinal flat mounts was performed according to Bruhn *et al.* (Bruhn and Cepko, 1996) with a few minor modifications. We used Scion

image software (Scion Corporation) to count the hybridization-positive signals. For serial sections, the hybridization was performed according to Wilkinson (1992) with a few minor modifications. The eyes were enucleated after orientation, and fixed in phosphate buffer (PB) containing 2% paraformaldehyde for 2 ~ 4 hours at 4°C. After being embedded in the OCT compound (Tissue-Tek), 7 μm frozen sections were collected. Hybridizations were carried out at 72°C for 18 hours, and posthybridization was conducted under highly stringent conditions. The probe was detected with alkaline phosphatase-conjugated antibody to digoxigenin. For immunostaining, 10 μm frozen sections were labeled with rabbit polyclonal anti-mouse Green opsin antibody (1:1000, MBL, Nagoya), and then were incubated with Alexa Fluor 546 goat anti-rabbit IgG (Molecular Probes) to reveal the primary antibody.

RESULTS

Molecular properties of the mouse Green S308A pigment

Wild-type mice having *S* and *L* cone pigments are maximally sensitive to UV (355 nm) and Green (508 nm) lights, respectively (Sun *et al*., 1997; Yokoyama *et al*., 1998), and show dichromatic color vision (Jacobs *et al*., 1991, 2004; Lyubarsky *et al*., 1999). We focused on the Ser/Ala at position 308 (Sun *et al*., 1997) of the *L* pigment, because this substitution exhibited the largest spectral shift among previously reported amino acid residues responsible for spectral tuning of *L* pigments (Yokoyama and Yokoyama, 1990;

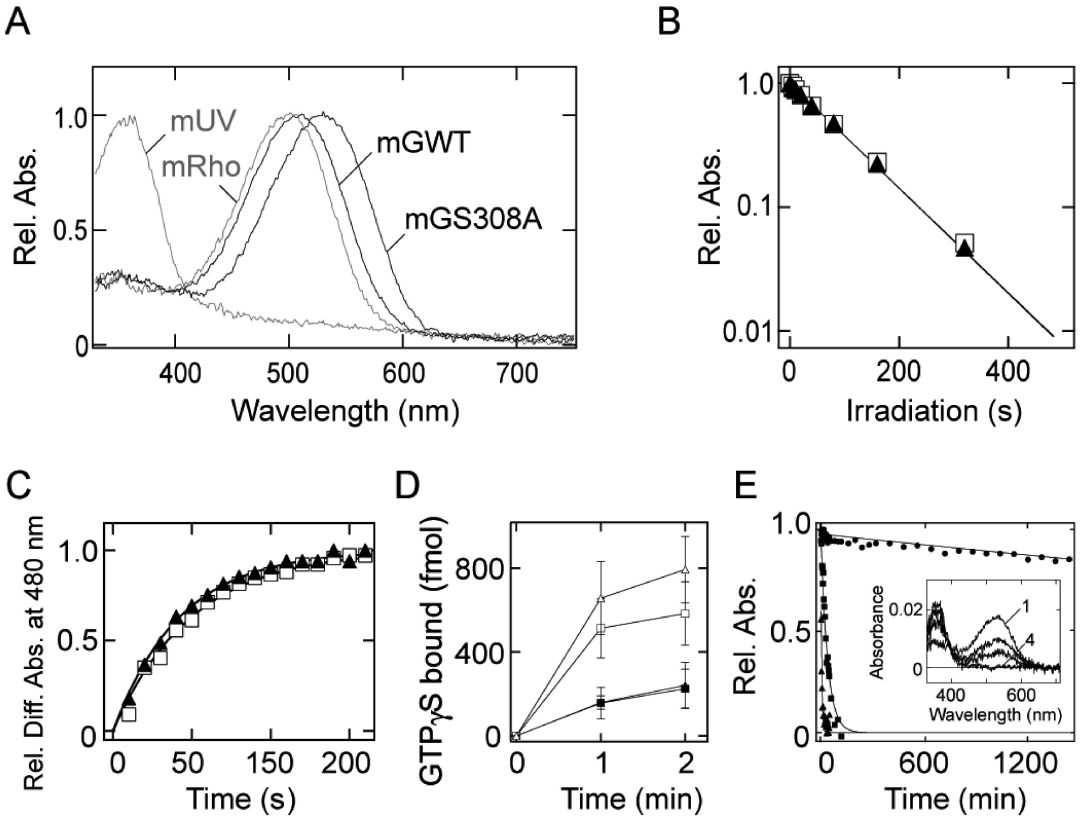

Fig. 1. Molecular properties of mouse Green wild-type and S308A pigments. **A**: Absorption spectra of pigments solubilized by the buffer supplemented with 0.75% CHAPS and 0.8 mg/ml PC and purified by an antibody-conjugated column. Absorption maxima (λ_{max}) of UV pigments (mUV), rhodopsin (mRho), wild-type Green (mGWT), and the S308A (mGS308A) were located at 360 nm, 500 nm, 510 nm, and 534 nm, respectively. **B**: Photosensitivity of mGWT (*square*) and mGS308A (*triangle*) at 520 nm. The pigments were irradiated with a 520 nm light in the presence of 1 mM hydroxylamine at 2°C. The decreases in absorbance at 520 nm were then plotted as functions of the irradiation time. The data points were fitted with exponential curves with time constants of 103 s (mGWT) and 102 s (mGS308A), respectively. Note that the ratio of time constants correlated relative photosensitivities between the two pigments and it is evident from the values that these two pigments exhibited identical photosensitivities. **C**: Course of thermal conversion from meta-II to meta-III intermediates of mGWT (*square*) and mGS308A (*triangle*). The pigment samples (0.04 O.D.) were irradiated with yellow light (>540 nm) at 2°C, and increases in absorbance at 480 nm due to the formation of meta-III from meta-II were plotted. The data points were fitted with exponential curves. The time constants were 50±9.3 s (n=3) in mGWT and 42±6.4 s (n=3) in mGS308A, respectively. **D**: Time-course of G-protein activation of mGWT (*square*) and mGS308A (*triangle*) at 4°C. A radionucleotide filter binding assay, which measures a light-dependent GDP/GTPγS exchange by G protein, was carried out. The amount of GTPγS-bound transducin of un-irradiated (closed symbols) and irradiated pigments (open symbols) were plotted. **E**: Hydroxylamine sensitivities of mGWT (*square*), mGS308A (*triangle*) and mRho (*circle*). Absorption spectra of the pigments were continuously recorded after addition of a neutralized hydroxylamine (100 mM final concentration) into the pigment samples at 20°C. The decrease in absorbance at λ_{max} was plotted against time after addition of hydroxylamine. The lines are the fitted exponential curves with time constants of 38.5 min (mGWT), 4.8 min (mGS308A) and 10819 (mRho) min, respectively. The inset shows four representative spectra taken before and after the addition of hydroxylamine to the mGS308A sample. Trace 1, before addition of hydroxylamine; traces 2 to 4, 2.5 min, 5 min and 60 min after addition of hydroxylamine.

Neitz *et al*., 1991; Asenjo *et al*., 1994; Sun *et al*., 1997). The absorption spectrum and molecular properties of the S308A Green pigment were examined using a preparation expressed in cultured cells. First, we confirmed that the S308A (mGS308A) pigment exhibited an absorption maximum at 534 nm, which was 24 nm red-shifted from that of the wild-type (mGWT, 510 nm, Fig. 1A). Second, we confirmed that the photosensitivities of the pigments at 520 nm were identical with each other (Fig. 1B). It should be noted that 520 nm was the isosbestic point of the spectra of the two pigments when they were normalized at the maxima (Fig. 1A), indicating that these two pigments exhibited molecular extinction coefficients almost identical to each other (see the Method section). Third, we investigated the course of conversion from meta-II (G protein activating state) to meta-III by monitoring the changes in absorbance at 480 nm (Fig. 1C). The decay time constants of meta-II (and thus the formation rate of meta-III) in mGWT and mGS308A were 83±18 and 99±17 s at 2°C, which were significantly smaller than that of mouse rhodopsin (4,170 s, data not shown). Fourth, we examined light-induced G protein activation of mGWT and mGS308A, and found that the mGS308A exhibited G protein activation efficiency slightly but not significantly larger than that of mGWT (Fig. 1D), which was ~5 times less than that of rhodopsin (data not shown). Part of the reduced efficiency in wild-type was probably due to the fast decay of meta-II compared to that of rhodopsin (Imai *et al*., 1997; Starace and Knox, 1997; Babu *et al*., 2001; Tachibanaki *et al*., 2001; Das *et al*., 2004) as evidenced by spectroscopy (Fig. 1C). Finally, like other cone pigments, mGWT and mGS308A pigments were much more susceptible to high concentrations of hydroxylamine than rhodopsin and easily bleached in the dark (Fig. 1E). These results indicated that the point mutation at this position did not disturb the molecular properties of the Green pigment as a cone pigment. Based on this observation, we decided to generate the knock-in mice carrying the S308A substitution on the Green opsin allele (Fig. 2).

Knock-in constructs

The targeting vector (Fig. 2A, B) was electroporated into ES cell lines, and one of the 216 ES clones was identified as a homologous recombinant by G418, gancyclovir selection, and Southern blotting analysis (Fig. 2C). The knock-in mice were generated by blastocyst injection of the ES clones, and it was confirmed that the knock-in gene was viable and fertile. Since the targeted gene is X-linked, we hereafter refer to the two genotypes of hemizygous males as Sy and Ay (S, A, and y represent Ser, Ala, and Y-chromosome, respectively) and homozygous and heterozygous females as SS, SA, and AA. Here, Sy and SS represent genotypes of male and female wild-types, respectively, and

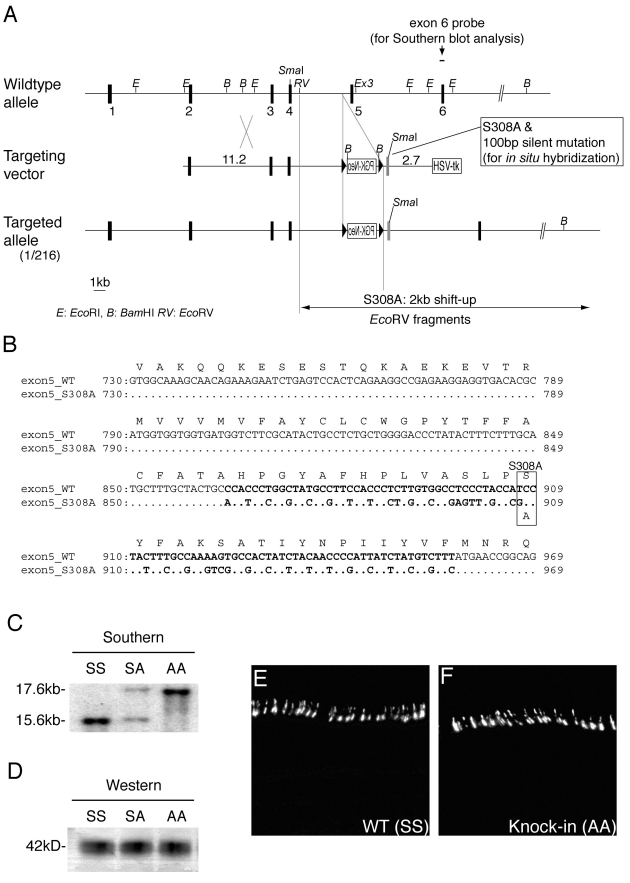

Fig. 2. Gene targeting to create the S308A knock-in mice. **A**: Diagram of homologous recombination (knock-in) to target the Green opsin allele. The filled boxes represent exons. Restriction endonuclease cleavage sites: *E*, *Eco*RI; *B*, *Bam*HI; *RV*, *Eco*RV. Scale bar, 1 kb. Upper: wild-type mouse Green gene allele. Middle: targeting vector. Gray box, targeted exon 5 including the S308A amino acid substitution and the 37 bp nucleotide substitution that do not change the amino acid sequences; PGK-Neo (reversed character) and filled triangles, a cassette of positive selection; HSV-tk, a cassette for negative selection. The numbers on both sides of exon 5 represent the lengths of linker genomic sequences. Lower: targeted allele. To identify homologous recombinants by Southern blot analysis, the exon 6 region (indicated by bar) was used for the franking probe. **B**: Alignments of the exon 5 sequences of wild-type (exon5_WT) and S308A (exon5_S308A). Dots indicate identical nucleotides. A deduced amino acid sequence of the exon5_WT is represented above the sequence. The boxed square represents codon 308, the Ser to Ala substitution that causes a 24 nm red-shift (this codon number is parallel to that of human Red). Bold characters represent nucleotide sequences including a 37 bp silent mutation that did not change the amino acid sequence. **C**: Southern blot of *Eco*RV-digested mouse-tail genomic DNA. The exon 6 probe (110 bp) detected a 15.6 kb fragment corresponding to wild-type (SS) and a 17.6 kb fragment corresponding to targeted allele (AA). SA mice carrying both alleles exhibit two bands. **D**: Western blot of protein extracts from 8-week mouse retinas. The polyclonal antibody for the 16-aa N-terminal of the mouse Green pigment detected both the wild-type and the S308A opsins in the 42 kD. The blotting intensities of SA and AA were not significantly different from SS. In **C** and **D**, there was no significant difference between samples from hemizygote males and homozygote females (Sy males and SS females, and Ay males and AA females). **E** and **F**: Immunostaining with the N-terminal antibody of the mouse Green pigment of SS (E) and AA (F) retinas.

SA is the heterozygote female that is expected to express three kinds of cone pigments with different spectral sensitivities.

To check the expression level of the knock-in protein, we performed Western blotting analysis of the retinal homogenates using an anti-mouse Green N-terminus antibody that recognizes both native and S308A pigments. The blotting patterns were similar in size and intensity among Sy/SS (WT), SA, and Ay/AA retinas (Fig. 2D). We also compared morphologies of entire retinas and cone cells between wild-type and knock-in mice. We could not find any differences in the thickness of retinal layers or the length of the cone outer segments (Figs. 2E and 2F). Therefore, we concluded that the introduction of the S308A substitution as well as the silent mutations did not affect retinal organization and development.

ERG measurements

To examine whether or not the photoreceptor cells expressing S308A pigments functioned properly, we recorded electroretinograms (ERG) of wild-type and knock-in mice by illumination with monochromatic lights (470 nm, 520 nm, and 570 nm) under conditions where rod-evoked responses were saturated by a background light. Since the amplitudes of the cone a-waves that resulted from photoreceptor hyperpolarization were too small to be quantified, we compared the response amplitudes of the cone b-waves, because the action spectrum for the cone-driven b-wave reflected the well-established UV and Green cone pigments (Jacobs *et al.*, 1991; Lyubarsky *et al.*, 1999).

Based on the absorption spectra of mGWT and mGS308A pigments (Fig. 1A), the response amplitude to 520 nm light should be larger than those to 470 nm and 570 nm lights in each genotype, and it should be equivalent among the genotypes because the two pigments absorb 520 nm light equally. In fact, the response amplitudes of the b-wave to 520 nm light were indistinguishable between every genotype and larger than that evoked by other lights depending on the genotype (see Fig. 3A and its legend). In the Sy/SS (WT) mice, the response amplitude to 570 nm light was smaller than those to other two lights, while the latter two were similar. In Ay/AA mice, the response amplitude to 470 nm light was smaller than those to the other two lights. There was no difference in the response amplitude between hemizygote males and homozygote females. Because b-waves are mainly derived from ON bipolar cells, the response patterns of the amplitudes from these genotypes indicated that the spectral shift caused by the S308A pigment was processed to the second order neurons. In SA mice, the response amplitudes to 470 nm and 570 nm lights were equivalent.

To quantify the spectral sensitivity altered by the expression ratio of native and S308A pigments, b-wave amplitude ratios (470/520 and 570/520), normalized by the isosbestic point (520 nm, Fig. 1A), were compared. The ratio averages in the SA mice were placed in the middle of the ratio averages of Sy/SS (WT) and Ay/AA (Fig. 3B). In addition, there were no significant differences in the value of variance among Sy/AA (WT), SA and Ay/AA (see legend in Fig. 3B), suggesting that individual variation in the ratio of native and S308A Green cones in the retinas of SA mice is not so large.

Ganglion cell responses

Next, we examined the light responses of ganglion cells under the whole cell clamp. The rod inputs were saturated by the background light. The three monochromatic lights used in ERG recording were applied as light stimuli after calibrating their photon flux densities. The intensities of background and stimulus lights in this experiment were equivalent to those previously used in usual cone ERG recordings (Lyubarsky *et al.*, 1999).

We randomly selected cells located in the ganglion cell layer. The recorded cells were categorized into ganglion cells (ON, OFF, and ON-OFF types) and displaced amacrine cells based on the waveform of excitatory postsynaptic current (EPSC) and spikes during illumination (Matsui *et al.*, 2001). Of approximately 30 cells examined for each genotype, we analyzed the responses of ON transient type ganglion cells in each genotype. The dendritic fields of recorded cells revealed by Lucifer yellow staining were approximately 150 μm in diameter in all genotypes. Therefore, it is likely that the analyzed cells may belong to a homogeneous morphological class.

Fig. 3C shows typical current responses of ON transient ganglion cells under the voltage clamp. Responses reached a peak at 20 ~ 50 ms after the onset of light and decayed to a sustained level during 500 ms illumination. There was some relationship between the response profile measured in current clamp mode and that measured in voltage clamp mode. That is, spike frequency in the current clamp mode (Fig. 3C, bottom traces) reflected the amplitude of current responses (Fig. 3C, upper three traces). Therefore, we examined the peak amplitudes of the current responses evoked by different wavelengths in the voltage clamp mode in detail. In most cells, the largest response was evoked by the 520 nm light. This observation is consistent with the data that the 520 nm absorbance is higher than the 470 nm or 570 nm absorbances in both mGWT and mGS308A Green pigments. In the Sy/SS (WT) mice, the 470 nm light evoked a larger peak amplitude and a higher spike frequency (data not shown) than the 570 nm light, while in the Ay/AA mice, the 570 nm light evoked larger responses (Fig. 3C). The ratios of peak amplitudes evoked by 470 nm and 570 nm to that evoked by 520 nm (470/520 and 570/520) were scattered compared with those measured in ERG. This is probably due to the difference in subtypes of ON transient ganglion cells (Kong *et al.*, 2005) or feedback/forward modification in inner plexiform layer cells (Lukasiewicz and Shields, 1998; Roska *et al.*, 2000; Matsui *et al.*, 2001). There were no differences in response properties between hemizygote males and homozygote females. The response

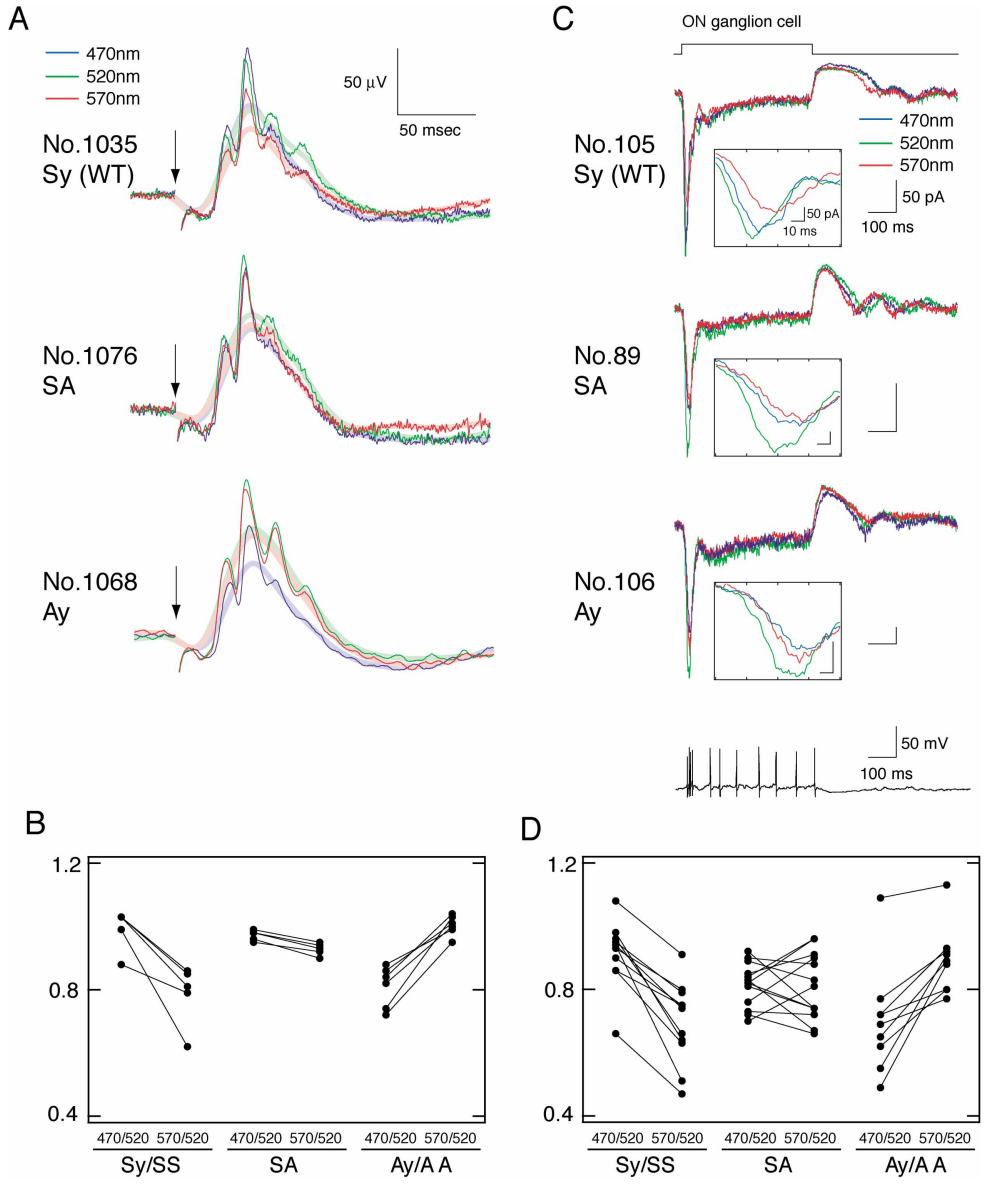

Fig. 3. Electroretinogram and patch clamp ganglion cell recordings evoked by 470 nm, 520 nm, and 570 nm monochromatic light stimuli. **A**: Typical response families of ERG in genetically identified Sy/SS (WT), SA, and Ay/AA mice. The arrows represent light flashes. Each trace is the average of 30 ~ 40 individual responses. The smooth and thick pastel trace corresponding to each curve color was obtained by a digitally averaged response with a Gaussian filter with σ=8 ms (bandwidth 16.6 Hz at 3 dB cutoff). The b-wave responses were calculated by subtracting the maximum value (b-wave) from the minimum value (a-wave) of the filtered traces. The averages±SD of the amplitude evoked by 520 nm light were 116±17 μV, 115±30 μV and 129±27 μV for Sy/SS (n=6), SA (n=5), and Ay/AA (n=6), respectively. It should be noted that the responses of the UV cone were enhanced in this background light condition. This resulted in the enhancement of response to 470 nm blue light in all genotypes compared to the expected amplitude calculated from the spectra of the pigments. **B**: The ratios of the b-wave amplitudes evoked by the 470 nm and 570 nm light stimuli were normalized to that of the 520 nm (isosbestic point of the two pigments) light stimulus. The values of 470/520 were 1.01±0.05, 0.95±0.05 and 0.82±0.06 for Sy/SS (n=6), SA (n=5), and Ay/AA (n=6), respectively. The values of 570/520 were 0.81±0.07, 0.92±0.04 and 0.99±0.03 for Sy/SS, SA, and Ay/AA, respectively. A Student's t-test between the Sy/SS and Ay/AA ratios showed significant levels (p<0.001), and an ANOVA test of all genotypes showed a significant difference (p<0.005). An F-test between the variances of 470/520 in Sy/SS and SA showed a significant level (p=0.01), but an F-test between the variances of 570/520 in Ay/AA and SA did not show a significant level (p=0.17). **C**: Typical current traces from ON ganglion cells from the Sy/SS (WT, No. 105), SA (No. 89), and Ay/AA (No. 106) mice. Horizontal and vertical scale bars indicate 100 ms and 50 pA, respectively. The top trace illustrates the light stimulus (500 ms). The bottom trace indicates the spike train recorded from the Ay/AA cell under a current clump. The insets show enlarged current traces around the peak amplitudes (30 ms ~ 70 ms). D: Peak amplitude ratios of responses generated by three monochromatic lights of each ganglion cell examined. The average±SDs of 470/520 were 0.91±0.10, 0.81±0.07, and 0.70±0.16 for Sy/SS (n=11), SA (n=13), and Ay/AA (n=9) mice, respectively. The values of 570/520 were 0.70±0.12, 0.81±0.10, and 0.89±0.10 for Sy/SS, SA, and Ay/AA mice, respectively. The difference between Sy/SS and Ay/AA ratios was quite significant (p<0.002; Student's t-test). The difference among all genotypes was also significant (p<0.005).

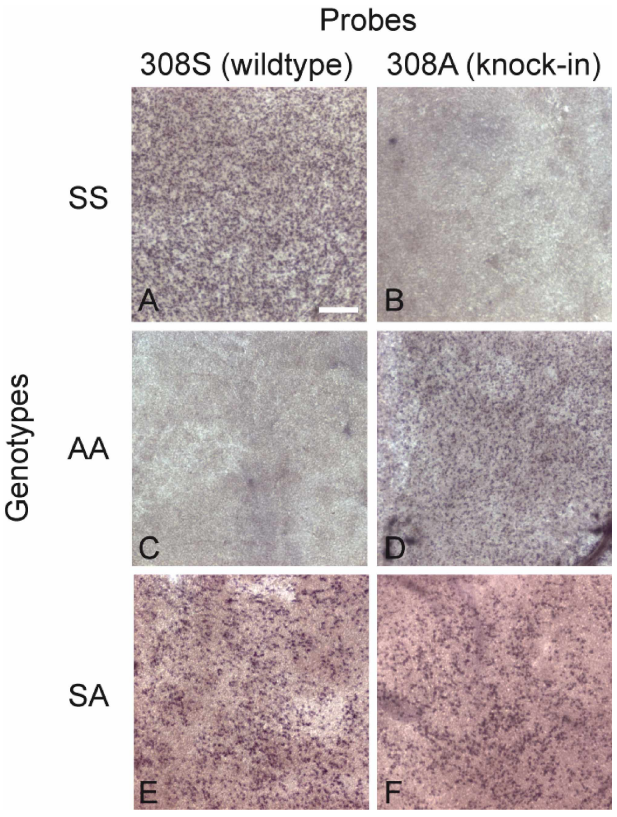

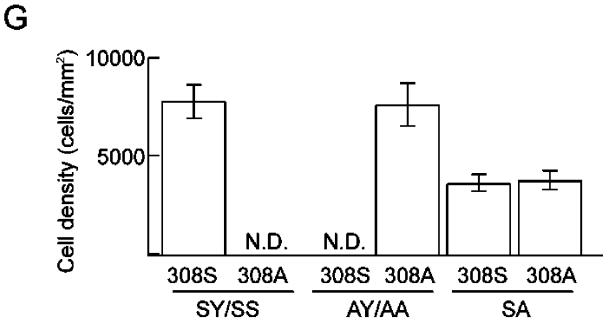

Fig. 4. Spatial distribution of the native and S308A Green cone cells in SA retinas. To visualize the expression patterns of the two mRNAs, *in situ* hybridization was performed using retinal flat mounts from 8-week mice (**A**–**F**). Hybridization images were taken from the dorsal regions of the retinas. Two 160 bp probes that were specific to wild-type and the S308A mRNA were hybridized. The first (**A**, **C**, and **E**) and the second (**B**, **D**, and **F**) columns represent hybridizations with the wild-type (308S) and the S308A (308A) specific probes, respectively. The scale bar: 100 μm. **G**: The average±standard deviation (SD) of signal densities of hybridization-positive cells from each genotype. In Sy/SS retinas, the value of 308S cells was 7773±849 cells/mm^2 (n=4). In Ay/AA retinas, the value of 308A cells was 7615±1091 cells/mm^2 (n=4). In SA, the values of 308S and 308A cells were 3636±435 cells/mm^2 and 3786±471 cells/mm^2 (n=4), respectively.

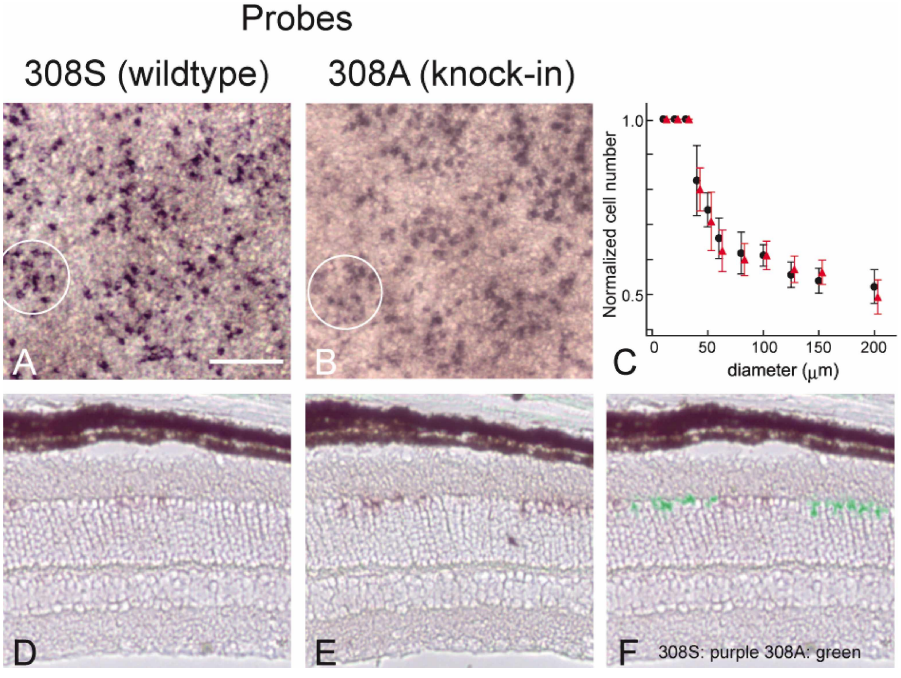

Fig. 5. Gene specific *in situ* hybridization in SA retinas using adjacent serial sections. **A** and **B**: Hybridization images of retinal flat mounts observed in a narrow field of view. Local assembly of hybridization signals in a diameter of approximately 30 μm was found. The white circle (30 μm in diameter) represents the local assembly of specific cone-types. **C**: Hybridization signal ratios of 308S (*circle*) and 308A (*triangle*) probes in SA mice normalized to that of SS mice. We scanned a circle in several diameters along the field of view of hybridization images (860×680 μm) and counted signals within the circle. The 5 highest values were averaged and normalized to those measured in SS mice. **D** and **E**: 7 μm serial sections from 8-week mice were hybridized with either 308S or 308A probes, respectively. The hybridization signals of each probe were not continuous. **F**: The merged image of **D** and **E** after conversion of the signal color of the S308A section to a green color. The image showed that the two hybridization signals did not overlap. The scale bar: 30 μm.

amplitude obtained from the SA mice was between that of the Sy/SS (WT) and Ay/AA mice, but whether 470 nm or 570 nm light evoked larger response varied in each ganglion cell examined. Namely, of the ganglion cells in SA retinas, there was no tendency for either 470/520 or 570/520 to become large (Fig. 3D). These facts suggest individual variance in cone inputs within the receptive field of ganglion cells examined.

Patch-like clusters of native and S308A Green cone cells in SA mice

Individual variance of spectral sensitivity in ganglion cells of SA retinas indicates that spatial distribution of specific cone-types is not uniform. Since the Green gene allele is X-linked, either gene is expressed in each cone cell by X-inactivation. In order to examine the expression of both opsin gene products in the SA mice, we visualized the two mRNAs by *in situ* hybridization.

For hybridization, 100 bp regions around codon 308, where the 37 bp silent nucleotide mutation was inserted, were used as the probe to separately visualize wild-type and S308A mRNAs. Since the hybridization signal was found to be weak with the use of the 100 bp probe alone during the initial hybridization experiments, we appended a 60 bp fragment at the 5' side of exon 6 to the initial probe. After confirming probe specificity by dot blot hybridization, *in situ* hybridization was performed. In the retinal flat mounts from the SS and AA retinas, hybridization signals were only detected in the specific probes (Figs. 4A–D), indicating that the probes were specifically hybridized (hybridization stringency; see Materials and Methods). Intensities of the two hybridization-positive signals were dorsal-ventral gradient, and the signal densities (Fig. 4G) obtained from hybridization-positive cells were similar to those reported previously (Jeon *et al*., 1998). In the SA retina, both hybridization signals emerged (Figs. 4E and 4F), and the number of hybridization-positive signals were halved compared to the Sy/SS (WT) and Ay/AA retinas (Fig. 4G).

Next, we investigated spatial distribution of specific cone-types in SA retinas. In expanded images of the retinal flat mounts (Figs. 5A and 5B), it was found that the hybridization signals from the same cone-types were not uniformly distributed. We therefore measured the cone density in a variety of ranges and normalized the number to that of the SS retinas (Fig. 5C). A circle of various diameters was scanned along the image, and hybridization positive signals within were counted. The five highest values were averaged, which represents the highest cone density of each range. As a result, the value measured in the large range was almost 0.5, while the value was one when measured up to 30 μm diameter. This observation indicated that the cone density of specific cone-types was equivalent between SS/AA and SA retinas within 30 μm in diameter and that local assembly of specific cone-types existed. To evaluate the spatial distribution more precisely, adjacent serial sections (7 μm) were stained with either of the two probes (Fig. 5D and 5E), and the images were merged (Fig. 5F). The signals did not overlap, indicating that either native or S308A pigment was expressed in each cone cell due to X- inactivation. In addition, the signals of one cone-type formed patch-like clusters that were exclusive from another cone-type. The local assembly derived from X-inactivation was reported as in rod cells (rod columnar mosaics), which was visualized by transgenic mice with *lac*Z reporter gene on X-chromosome (Reese *et al*., 1995). Since each columnar mosaic resulted from proliferation of the rod precursor after X-inactivation, the patch-like clusters in this study would be generated by the similar developmental mechanism. It is suggested that spatial distribution contributes to the individual variance observed in ganglion cell recording from SA retinas.

DISCUSSION

In the present study, we introduced a S308A amino acid substitution into the wild-type *L* opsin (Green) gene. While the λ_{max} of the pigment was 24 nm red-shifted by the mutation, other pigment properties including photosensitivity were not so disturbed (Fig. 1). Furthermore, there were no differences in the length of the outer segments and the retinal layer morphology between wild-type and knock-in mice. These results suggested that sufficient efficiency in the phototransduction cascade was achieved in mutant cone cells as in wild-type. In fact, amplitudes of ERG evoked by 520 nm (isosbestic point) light were identical between Sy/SS (WT) and Ay/AA mice (Fig. 3A). However, the amplitudes of ERG evoked by 470 nm and 570 nm light reflected the spectral properties of the pigments contained in the respective mice. These observations clearly showed that the S308A pigments can function in the photoreceptor cells as red-shifted *L* pigments. Therefore, we successfully generated knock-in mice having two kinds of cone cells that exhibited different spectral sensitivity.

Since the Green gene is located on the X-chromosome, the cone cells of the heterozygote (SA) females should express either wild-type or S308A Green pigments randomly, because there is no maternal/paternal preference in X-inactivation in retinas (Mollon *et al*., 1984). In fact, the response ratios (470/520 and 570/520) of ERG were midway between those of Sy/SS (WT) and Ay/AA, and the SD values were equivalent to those of Sy/SS and Ay/AA. This result indicated that the number of cells of native and S308A Green cone cells was almost equal, which was confirmed by the *in situ* hybridization (Fig. 4G). Also, this trend is consistent with previously reported data that about 50% of retinal cells are stained by X-gal in female mice carrying a *lac*Z transgene on a single X-chromosome (Reese *et al*., 1995, 1999; Reese and Tan, 1998; Reese and Galli-Resta, 2002).

ON ganglion cells of SA mice exhibited the largest responses when they were irradiated with 520 nm light, but the responses evoked by 470 nm or 570 nm irradiation relative to those evoked by 520 nm irradiation were variable in each cell. These observations could be due to the arrange-

ments of native and S308A Green cone cells in the retinas by X-inactivation. Because a cluster of respective cone cells was about 30 μm in diameter, which was shown by the hybridization images in Fig. 5, approximately 25 clusters would be included in the dendritic fields of the ganglion cells (150 μm in diameter). Thus the number of clusters of each cone-type covered by the ganglion cell was 8 ~ 16 out of the total number of the clusters (25), when the binominal probability distribution was set to the 95% range. In this case, each ganglion cell tended to show preference in convergence of native and S308A cone clusters. Our observation that amplitudes of response evoked by 470 nm and 570 nm lights were variable in each ganglion cell is in good agreement with the morphological data considering the local clusters of specific cone-types. If the cluster of each cone-type were not present, that is, each cone cell distributed randomly, the ratio of photosensitivity between 470 nm and 570 nm in each ganglion cell was 1: 1 within 95% binominal probability distribution. Therefore, the ganglion cell responses clearly showed the formation of cone clusters in the retinas of SA mice.

The native and S308A Green cone mosaics by X-inactivation were clearly visualized by *in situ* hybridization using specific probes for wild-type and S308A mRNAs. For such spatial distribution, it would be necessary for X-inactivation to occur before proliferation and migration of cone precursors. Cone cells are thought to be born between E11 and E15 (Carter-Dawson and LaVail, 1979), and develop from ventricular cells when a long vitreal process fails to develop following final mitosis (Hinds and Hinds, 1979). On the other hand, transcription of *Xist*, which is thought to be a trigger gene of X-inactivation, is found at E12.5 in outer neuroblastic layer where cone progenitors are located (Blackshaw *et al.*, 2004). In addition, transcription of photoreceptor specific nuclear receptor *Nr2e3* is found from E16.5 (Cheng *et al.*, 2004) that is considered to suppress cone proliferation (Chen *et al.*, 2005). Therefore, the cone clusters would be generated by X-inactivation after E14 and hereafter proliferation of cone precursor occurs until E18.

In order to investigate the molecular basis of color vision in primates, the use of genetically engineered mice has been reported. First, transgenic mice with human Red cDNA were generated (Shaaban *et al.*, 1998), where the Red pigments are co-expressed in all cone cells. These experiments also showed that the expressed pigments can function as the native pigments in the cells to broaden the spectral sensitivities of the cone cells. Then, during the course of our electrophysiological experiments, there were reports of knock-in mice whose Green gene locus was partially replaced by human Red cDNA (Smallwood *et al.*, 2003). In their knock-in construct, the 3' portion of the human Red cDNA (corresponding to amino acids 98–364 in the human numbering system) was introduced into the exon 2 of the mouse Green locus, that is, they disturbed the exon-intron arrangement from exon 2 to 6. They showed that the knock-in Red pigment is expressed in respective cone cells exclusively from the native Green pigments, but, in multi-electrode recordings, responses derived from native Green cone cells are dominant in the heterozygotes. The amplitude of the ERG responses shows large individual variance in the ratio of Red:Green cone cells. Since the variance was not observed in our knock-in mice, the difference may be ascribed to the difference in knock-in construct.

Our knock-in mice expressed two kinds of *L* cone pigments with distinct spectral sensitivities in a mutually exclusive manner in respective cone cells due to random X-inactivation in retinal cells as seen in New World primates. It was reported that, in wild-type mice, UV (*S*) and Green (*L*) opsins are co-expressed in cone cells and that the degree of expression shows spatial gradient in the dorsal-ventral coordinate (Applebury *et al.*, 2000). However, our recent investigations showed that cone cells expressing only *L* pigments dominated in the dorsal half of retinas and that most UV-expressing cone cells contained less than 10% *L* pigments (UV dominant) (AO, HI and YS, unpublished data). Therefore, it is expected that in the dorsal halves of retinas in SA mice, three kinds of cone cells exist: UV, native Green and S308A Green. Unlike the anthropoid retina, the mouse retina has no fovea, thus the arrangement of three kinds of cone cells with different spectral sensitivities in the retinas of the knock-in mice would be similar to that found in the peripheral region of the retinas of New World primates. Although spatial distribution of two polymorphic *L* cone cells has not been reported in the peripheral retinas in New World primates thus far, our observation in SA mice strongly suggested the presence of the cone cell clusters in the New World primates due to X-inactivation machinery. The morphology and physiology of retinal ganglion cells are similar in New and Old World primates (reviewed in Silveira *et al.*, 2004), and their dendritic fields are similar to those we observed in the mice. In the macaque peripheral retina (20 ~ 50° of eccentricity), Martin *et al.* (2001) found that 80% of midget ganglion cells are color opponent, which is consistent with a "selective connection" model (Lee *et al.*, 1998; Martin *et al.*, 2001; Kolb and Marshak, 2003) of Red-Green opponency that hypothesizes cone type-specific connections. It is plausible that the opponency emerges in the peripheral retina of the New World primates due to the cone type-specific patches generated by X-inactivation. Thus our mice would be one of the models for exploration of the genes and proteins responsible for the opponency in peripheral retina of the New World primates. Also, our mice can be used as a model for elucidation of the evolution of visual systems from mammals to primates.

ACKNOWLEDGMENTS

This work was supported in part by grants from the Ministry of Education, Culture, Sports, Science, and Technology (MEXT) to H. I. and Y. S., by the Grant for Biodiversity Research of the 21st Century COE (A14), and by research fellowships from the Japan Society for the Promotion of Science for Young Scientists to A. O. We thank Dr. S. Koike for providing us with the 293T cell lines and Prof.

R. S. Molday for the gift of rhodopsin 1D4-producing hybridoma. We also thank Dr. S. Kuwayama for technical advice on spectroscopy, Ms. H. Watanabe for technical assistance on blastcyst injection, and Drs. Y. Miyake, M. Kondo, S. Ueno, and Mr. N. Tammitsu for technical advice on ERG.

REFERENCES

Applebury ML, Antoch MP, Baxter LC, Chun LL, Falk JD, Farhangfar F, Kage K, Krzystolik MG, Lyass LA, Robbins JT (2000) The murine cone photoreceptor: a single cone type expresses both S and M opsins with retinal spatial patterning. Neuron 27: 513–523

Asenjo AB, Rim J, Oprian DD (1994) Molecular determinants of human red/green color discrimination. Neuron 12: 1131-1138

Babu KR, Dukkipati A, Birge RR, Knox BE (2001) Regulation of phototransduction in short-wavelength cone visual pigments via the retinylidene Schiff base counterion. Biochemistry 40: 13760–13766

Blackshaw S, Harpavat S, Trimarchi J, Cai L, Huang H, Kuo WP, Weber G, Lee K, Fraioli RE, Cho S-H *et al*. (2004) Genomic Analysis of Mouse Retinal Development. PLoS Biol 2: e247

Bruhn SL, Cepko CL (1996) Development of the pattern of photoreceptors in the chick retina. J Neurosci 16: 1430–1439

Calkins DJ, Tsukamoto Y, Sterling P (1998) Microcircuitry and mosaic of a blue-yellow ganglion cell in the primate retina. J Neurosci 18: 3373–3385

Carter-Dawson LD, LaVail MM (1979) Rods and cones in the mouse retina. II. Autoradiographic analysis of cell generation using tritiated thymidine. J Comp Neurol 188: 263–272

Chan TL, Martin PR, Clunas N, Grunert U (2001) Bipolar cell diversity in the primate retina: morphologic and immunocytochemical analysis of a new world monkey, the marmoset *Callithrix jacchus*. J Comp Neurol 437: 219–239

Chen J, Rattner A, Nathans J (2005) The rod photoreceptor-specific nuclear receptor Nr2e3 represses transcription of multiple cone-specific genes. J Neurosci 25: 118–129

Cheng H, Khanna H, Oh ECT, Hicks D, Mitton KP, Swaroop A (2004) Photoreceptor-specific nuclear receptor NR2E3 functions as a transcriptional activator in rod photoreceptors. Hum Mol Genet 13: 1563–1575

Chisaka O, Capecchi MR (1991) Regionally restricted developmental defects resulting from targeted disruption of the mouse homeobox gene hox-1.5. Nature 350: 473–479

Dacey DM (1996) Circuitry for color coding in the primate retina. Proc Natl Acad Sci USA 93: 582–588

Dacey DM, Lee BB (1994) The 'blue-on' opponent pathway in primate retina originates from a distinct bistratified ganglion cell type. Nature 367: 731–735

Das J, Crouch RK, Ma JX, Oprian DD, Kono M (2004) Role of the 9-methyl group of retinal in cone visual pigments. Biochemistry 43: 5532–5538

Ghosh KK, Goodchild AK, Sefton AE, Martin PR (1996) Morphology of retinal ganglion cells in a new world monkey, the marmoset Callithrix jacchus. J Comp Neurol 366: 76–92

Goodchild AK, Martin PR (1998) The distribution of calcium-binding proteins in the lateral geniculate nucleus and visual cortex of a New World monkey, the marmoset, Callithrix jacchus. Vis Neurosci 15: 625–642

Hanazawa A, Mikami A, Sulistyo Angelika P, Takenaka O, Goto S, Onishi A, Koike S, Yamamori T, Kato K *et al*. (2001) Electroretinogram analysis of relative spectral sensitivity in genetically identified dichromatic macaques. Proc Natl Acad Sci USA 98: 8124–8127

Hemmi JM, James A, Taylor WR (2002) Color opponent retinal ganglion cells in the tammar wallaby retina. J Vis 2: 608–617

Hinds JW, Hinds PL (1979) Differentiation of photoreceptors and horizontal cells in the embryonic mouse retina: an electron microscopic, serial section analysis. J Comp Neurol 187: 495–511

Hong K, Hubbell WL (1972) Preparation and properties of phospholipid bilayers containing rhodopsin. Proc Natl Acad Sci USA 69: 2617–2621

Imai H, Terakita A, Tachibanaki S, Imamoto Y, Yoshizawa T, Shichida Y (1997) Photochemical and biochemical properties of chicken blue-sensitive cone visual pigment. Biochemistry 36: 12773–12779

Imai H, Terakita A, Shichida Y (2000) Analysis of amino acid residues in rhodopsin and cone visual pigments that determine their molecular properties. Methods Enzymol 315: 293–312

Jacobs GH, Neitz J (1985) Color vision in squirrel monkeys: sex-related differences suggest the mode of inheritance. Vision Res 25: 141–143

Jacobs GH, Neitz J, Deegan JF 2nd (1991) Retinal receptors in rodents maximally sensitive to ultraviolet light. Nature 353: 655–656

Jacobs GH, Neitz M, Deegan JF 2nd, Neitz J (1996) Trichromatic colour vision in New World monkeys. Nature 382: 156–158

Jacobs GH, Williams GA, Fenwick JA (2004) Influence of cone pigment coexpression on spectral sensitivity and color vision in the mouse. Vision Res 44: 1615–1622

Jeon CJ, Strettoi E, Masland RH (1998) The major cell populations of the mouse retina. J Neurosci 18: 8936–8946

Kolb H, Marshak D (2003) The midget pathways of the primate retina. Doc Ophthalmol 106: 67–81

Kong JH, Fish DR, Rockhill RL, Masland RH (2005) Diversity of ganglion cells in the mouse retina: Unsupervised morphological classification and its limits. J Comp Neurol 489: 293–310

Kuwayama S, Imai H, Hirano T, Terakita A, Shichida Y (2002) Conserved proline residue at position 189 in cone visual pigments as a determinant of molecular properties different from rhodopsins. Biochemistry 41: 15245–15252

Lee BB, Kremers J, Yeh T (1998) Receptive fields of primate retinal ganglion cells studied with a novel technique. Vis Neurosci 15: 161–175

Lukasiewicz PD, Shields CR (1998) Different combinations of GABAA and GABAC receptors confer distinct temporal properties to retinal synaptic responses. J Neurophysiol 79: 3157–3167

Lyubarsky AL, Falsini B, Pennesi ME, Valentini P, Pugh EN Jr. (1999) UV- and midwave-sensitive cone-driven retinal responses of the mouse: a possible phenotype for coexpression of cone photopigments. J Neurosci 19: 442–455

Mariani AP (1984) The neuronal organization of the outer plexiform layer of the primate retina. Int Rev Cytol 86: 285–320

Martin PR, Lee BB, White AJ, Solomon SG, Ruttiger L (2001) Chromatic sensitivity of ganglion cells in the peripheral primate retina. Nature 410: 933–936

Matsui K, Hasegawa J, Tachibana M (2001) Modulation of excitatory synaptic transmission by GABA(C) receptor-mediated feedback in the mouse inner retina. J Neurophysiol 86: 2285–2298

Mears AJ, Kondo M, Swain PK, Takada Y, Bush RA, Saunders TL, Sieving PA, Swaroop A (2001) Nrl is required for rod photoreceptor development. Nat Genet 29: 447–452

Mollon JD, Bowmaker JK, Jacobs GH (1984) Variations of colour vision in a New World primate can be explained by polymorphism of retinal photopigments. Proc R Soc Lond B Biol Sci 222: 373–399

Neitz M, Neitz J, Jacobs GH (1991) Spectral tuning of pigments underlying red-green color vision. Science 252: 971–974

Okano T, Kojima D, Fukada Y, Shichida Y, Yoshizawa T (1992) Primary structures of chicken cone visual pigments: vertebrate

rhodopsins have evolved out of cone visual pigments. Proc Natl Acad Sci USA 89: 5932–5936

Onishi A, Koike S, Ida M, Imai H, Shichida Y, Takenaka O, Hanazawa A, Komatsu H, Mikami A, Goto S *et al*. (1999) Dichromatism in macaque monkeys. Nature 402: 139–140

Onishi A, Koike S, Ida-Hosonuma M, Imai H, Shichida Y, Takenaka O, Hanazawa A, Komatsu H, Mikami A, Goto S *et al*. (2002) Variations in long- and middle-wavelength-sensitive opsin gene loci in crab-eating monkeys. Vision Res 42: 281–292

Reese BE, Galli-Resta L (2002) The role of tangential dispersion in retinal mosaic formation. Prog Retin Eye Res 21: 153–168

Reese BE, Tan SS (1998) Clonal boundary analysis in the developing retina using X-inactivation transgenic mosaic mice. Semin Cell Dev Biol 9: 285–292

Reese BE, Harvey AR, Tan SS (1995) Radial and tangential dispersion patterns in the mouse retina are cell-class specific. Proc Natl Acad Sci USA 92: 2494–2498

Reese BE, Necessary BD, Tam PP, Faulkner-Jones B, Tan SS (1999) Clonal expansion and cell dispersion in the developing mouse retina. Eur J Neurosci 11: 2965–2978

Roorda A, Metha AB, Lennie P, Williams DR (2001) Packing arrangement of the three cone classes in primate retina. Vision Res 41: 1291–1306

Roska B, Nemeth E, Orzo L, Werblin FS (2000) Three levels of lateral inhibition: A space-time study of the retina of the tiger salamander. J Neurosci 20: 1941–1951

Saito A, Mikami A, Hasegawa T, Koida K, Terao K, Koike S, Onishi A, Takenaka O, Teramoto M, Mori Y (2003) Behavioral evidence of color vision deficiency in a protanomalia chimpanzee (Pan troglodytes). Primates 44: 171–176

Sakmar TP, Franke RR, Khorana HG (1989) Glutamic acid-113 serves as the retinylidene Schiff base counterion in bovine rhodopsin. Proc Natl Acad Sci USA 86: 8309–8313

Schneeweis DM, Schnapf JL (1999) The photovoltage of macaque cone photoreceptors: adaptation, noise, and kinetics. J Neurosci 19: 1203–1216

Shaaban S, Crognale M, Calderone J, Huang J, Jacobs G, Deeb S (1998) Transgenic mice expressing a functional human photopigment. Invest Ophthalmol Vis Sci 39: 1036–1043

Shichida Y, Imai H (1998) Visual pigment: G-protein-coupled receptor for light signals. Cell Mol Life Sci 54: 1299–1315

Silveira LC, Saito CA, Lee BB, Kremers J, da Silva Filho M, Kilavik BE, Yamada ES, Perry VH (2004) Morphology and physiology of primate M- and P-cells. Prog Brain Res 144: 21–46

Smallwood PM, Olveczky BP, Williams GL, Jacobs GH, Reese BE, Meister M, Nathans J (2003) Genetically engineered mice with an additional class of cone photoreceptors: Implications for the evolution of color vision. Proc Natl Acad Sci USA 100: 11706–11711

Solomon SG (2002) Striate cortex in dichromatic and trichromatic marmosets: neurochemical compartmentalization and geniculate input. J Comp Neurol 450: 366–381

Starace DM, Knox BE (1997) Activation of transducin by a *Xenopus* short wavelength visual pigment. J Biol Chem 272: 1095–1100

Sun H, Macke JP, Nathans J (1997) Mechanisms of spectral tuning in the mouse green cone pigment. Proc Natl Acad Sci USA 94: 8860–8865

Tachibanaki S, Tsushima S, Kawamura S (2001) Low amplification and fast visual pigment phosphorylation as mechanisms characterizing cone photoresponses. Proc Natl Acad Sci USA 98: 14044–14049

Terakita A, Yamashita T, Tachibanaki S, Shichida Y (1998) Selective activation of G-protein subtypes by vertebrate and invertebrate rhodopsins. FEBS Letters 439: 110–114

Terao K, Mikami A, Saito A, Itoh S-i, Ogawa H, Takenaka O, Sakai T, Onishi A, Teramoto M, Udono T (2005) Identification of a protanomalous chimpanzee by molecular genetic and electroretinogram analyses. Vision Research 45: 1225–1235

Tovée MJ (1994) The molecular genetics and evolution of primate colour vision. Trends Neurosci 17: 30–37

Twig G, Levy H, Perlman I (2003) Color opponency in horizontal cells of the vertebrate retina. Prog Retin Eye Res 22: 31–68

Wienrich M, Zrenner E (1984) Cone mechanisms and their colour-opponent interaction in monkeys and cat. Ophthalmic Res 16: 40–47

Wilder HD, Grunert U, Lee BB, Martin PR (1996) Topography of ganglion cells and photoreceptors in the retina of a New World monkey: the marmoset Callithrix jacchus. Vis Neurosci 13: 335–352

Wilkinson DG (1992) *In Situ* Hybridization: A Practical Approach, Oxford University Press, New York

Yokoyama R, Yokoyama S (1990) Convergent evolution of the red- and green-like visual pigment genes in fish, *Astyanax fasciatus*, and Human. Proc Natl Acad Sci USA 87: 9315–9318

Yokoyama S, Radlwimmer FB, Kawamura S (1998) Regeneration of ultraviolet pigments of vertebrates. FEBS Lett 423: 155–158

(Received June 2, 2005 / Accepted September 2, 2005)